

Experimental study of the energy spectrum of the π^+ in $K^+ \rightarrow \pi^+ \pi^0 \pi^0$ decay*

M. Sheaff

Department of Physics, University of Wisconsin, Madison, Wisconsin 53706

(Received 7 April 1975)

A sample of 5635 π^+ with kinetic energies between 8 and 50 MeV was obtained from $K^+ \rightarrow \pi^+ \pi^0 \pi^0$ decays in the ANL-Michigan 40-in. heavy liquid bubble chamber filled with propane. For these the energy dependence was well described by a linear spectrum of the form $|M|^2 = 1 + g[(s_3 - s_0)/m_{\pi^+}^2]$, where $g = 0.602 \pm 0.021$. No evidence was found for a quadratic term significantly different from 0. When the five conventional test quantities for the isospin selection rules were formed using the value of g from this experiment and current world averages for the other $K \rightarrow 3\pi$ decay parameters, it was found that there was significant evidence for $|\Delta I| = 3/2$ amplitudes into both $I = 2$ and $I = 1$ final states. These experimental values are in good agreement with theoretical predictions for them obtained in models which satisfy the current-algebra relation at the soft-pion points and include $|\Delta I| = 3/2$ as well as $|\Delta I| = 1/2$ amplitudes.

I. INTRODUCTION

We have studied the structure of the decay spectrum of the charged secondary in the τ' decay mode of the K^+ , $K^+ \rightarrow \pi^+ \pi^0 \pi^0$. The number of events after cuts was 5635, which, while low in statistics compared to experiments involving $K^+ \rightarrow \pi^+ \pi^+ \pi^-$ and $K_L^0 \rightarrow \pi^+ \pi^- \pi^0$, represents the largest sample of τ' data reported to date.

The experiment was performed in the ANL-Michigan 40-in. heavy liquid bubble chamber (HLBC) filled with propane in a magnetic field of 41.5 kG. The combination of high field and long-radiation-length liquid in a relatively large-volume heavy liquid bubble chamber enabled us to reduce all backgrounds and geometric corrections significantly and to accurately estimate those that remained, primarily by using information obtained experimentally rather than relying on theoretical calculations. Thus the final result does not depend in a very important way on Monte Carlo calculations, which reduces the possibility of hidden systematic errors. A further advantage of our experiment comes from a careful accounting of all events. Only 1.4% of the events, which failed for reasons unrelated to the π^+ energy, were ignored at the analysis stage. All others were forced through analysis and included in the sample.

Motivation for the experiment was provided by the fact that the τ' is the least studied of the $K \rightarrow 3\pi$ decays, for which comparison of the coefficient of the term linear in the odd pion energy, according to a suggestion first proposed by Weinberg,¹ provides a sensitive test for the presence of amplitudes with $|\Delta I| > \frac{1}{2}$.²

II. EXPERIMENTAL INFORMATION

The results reported here are from an exposure of 132 000 pictures containing approximately 8.3×10^5 stopping K^+ , or an average of 6.3 K^+ /picture, in the ANL-Michigan 40-in. heavy liquid bubble chamber at the Argonne National Laboratory Zero-Gradient Synchrotron (ZGS). The 28° separated K^+ beam at a momentum of 800–850 MeV/c was degraded by a copper absorber at the chamber window, so that the K^+ 's stopped, for the most part, well within the chamber volume. The chamber was filled with propane at a density of 0.428 g/cm³. The density was determined experimentally for our exposure using 50 kinematically fitted pions from the top of the τ spectrum, and the range-momentum curve was calibrated accordingly.

The film was scanned twice for decays to a single charged secondary according to the following criteria:

(1) The K^+ was to appear to stop both by ionization and curvature. A template was provided for the curvature test, and if the K^+ appeared to be straighter than the template in all 3 views, it was rejected. To ensure an adequate length of track for the template curvature test and for calculation of momentum by curvature, which is used in a further test on stopping which will be described later, no K^+ 's with a scatter $> 30^\circ$ in the last 15 cm were accepted.

(2) The secondary was required to have curvature and ionization consistent with a stopping pion and to stop within the range of a template provided. The range of the template extended to 25 cm in a real space, the maximum range of a

stopping τ' pion being 22 cm, to prevent a scan bias at the top of the spectrum and to provide a small region above the spectrum for background consistency checks. π^+ secondaries with a scatter $> 30^\circ$ were rejected since most collisions involving large energy losses occur at angles larger than 30° . This results in an energy-dependent correction to be discussed in the section on corrections to the data.

(3) The π - μ - e chain was required to be visible, visible meaning two distinct changes in angle ≤ 3 mm apart at the end of the π^+ . The 3 mm range is actually about $1\frac{1}{2}$ times the true μ range from stopping π decay and was chosen long enough to include all true π - μ - e and to set a definite criterion for the subsample of $K_{\mu 3}$ events which appeared to have typical π - μ - e endings. (In what follows, these typical π - μ - e endings will be referred to as " μ pips.")

Each event found was re-examined by either a professional scanner with ten years experience at similar heavy liquid K^+ experiments or by the writer to check that it did indeed meet the criteria. In all, 8 143 events were accepted for measurement.

At the completion of each roll, about 50 $K_{\mu 2}$ decays were selected, to determine the percentage of these which fit criterion (3). The percentage averaged over all rolls was then used as one means of estimating the background due to $K_{\mu 3}$ with false π - μ - e endings.

The average single-scan efficiency was found to be 76.8%, giving an estimated double-scan efficiency of 95.2%. It is the double-scan efficiencies for the individual energy bins which are of real interest in this experiment, since if these tend to be higher at one end of the spectrum than at the other, the spectrum will be biased. Figure 1 shows the double-scan efficiencies by energy bin with errors. Since the efficiencies tend to be lower at both ends than at the center, the shift in the slope resulting from the difference in efficiencies across the spectrum is only $+0.002$, which is much smaller than the statistical error.

Each of the 8 143 events accepted was measured on an image plane digitizer and reconstructed in real space by the HLBC program SHAPE. All events were measured at least twice in an attempt to get as many as possible to pass measurement.

All but 480 events (5.9%) passed measurement. Out of this sample, 72 were lost through book-keeping errors or computer tape failures, and another 40 through failure of the K^+ track to reconstruct. Since these were presumably unbiased as to π^+ energy, they were discarded. The remaining events, 200 π^+ track failures and 168

vertex reconstruction failures, were retained. 126 of these events had sufficient information from the reconstruction to determine range and dip angle; for the remainder, the range and dip were measured by an on-line measuring table program (RANGER), which was calibrated against SHAPE for a sample of good events. In all, 235 events fell within the range and dip limits and were included in the data sample. As they were heavily biased toward short tracks, their elimination would have significantly reduced the magnitude of the slope obtained.

III. CUTS AND CORRECTIONS TO THE DATA

A. Cuts

(i) K^+ 's which had a dip angle of greater than $\pm 30^\circ$ with respect to the window were eliminated, a total of 102 events.

(ii) To eliminate K^+ decays in flight, momentum measurements by range and curvature were compared. The limits set were

$$-14 \text{ MeV}/c < p_{\text{range}} - p_{\text{curv}} < 30 \text{ MeV}/c.$$

793 events were eliminated by this test, many of which were probably stopping K^+ events. The loss of good events was small compared to the

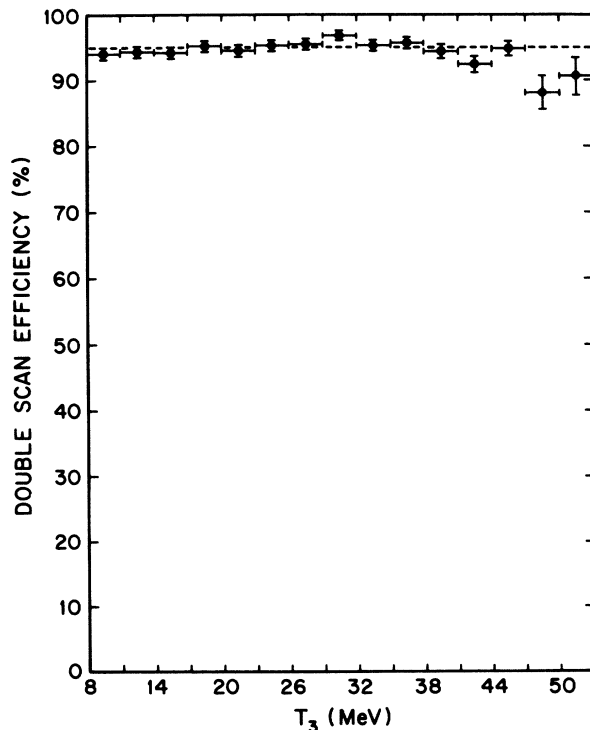


FIG. 1. Double-scan efficiency versus kinetic energy of the π^+ .

total number and was well justified by the resulting accuracy to which the in-flight contamination could be estimated. A sample of τ events was measured and subjected to kinematic fitting for comparison. Of the 842 events which survived this cut, all of which would have been accepted as stopped using the scanning template, 23, or 2.73%, fitted the τ -in-flight hypothesis. The K^+ momentum distribution for these fitted events, shown in Fig. 2, was used in estimating the K_{π^2} - and τ' -in-flight corrections to the data.

(iii) 876 events were cut because the π^+ range was shorter than 0.81 cm (< 8 MeV) or longer than 21.76 cm (> 53 MeV), the maximum τ' range.

(iv) 381 events were rejected as having π^+ dip greater than ± 1.2 radians. Figure 3 shows the distribution in dip cosine for 5360 of the 5635 events included in the final spectrum analysis. As expected, the distribution is flat within statistics indicating that there is no loss of events within the cut region and therefore no range bias introduced by this cut.

(v) 106 events were eliminated because the K^+ decay origin was less than 4 cm from the top or bottom of the chamber or less than 5 cm from the perimeter. This cut was chosen to reduce corrections for π^+ escape from the visible chamber volume. The resulting correction [see Sec. III B (vi)] is only 4% at the top of the spectrum and drops rapidly for shorter tracks.

The angle between the K^+ direction and π^+ direction at the vertex was computed for each event.

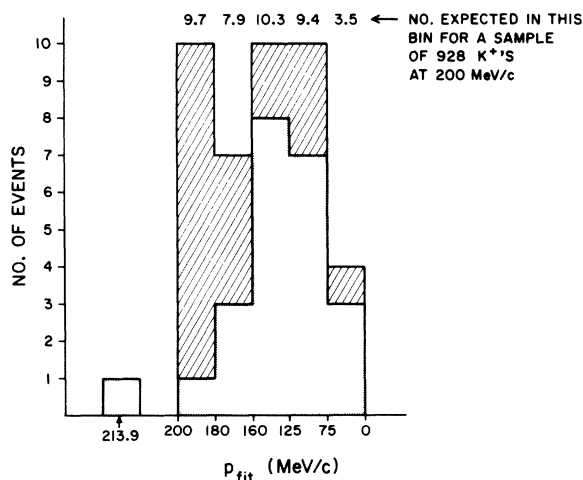


FIG. 2. Momentum distribution of K^+ 's from fitted τ -in-flight events—the shaded region contains the K^+ 's that passed the K^+ -at-rest test ($-14 < p_{range} - p_{curv.} < +30$ MeV/c) and the cross-hatched region those that did not ($p_{range} - p_{curv.} < -14$ MeV/c).

A cut was contemplated for π^+ 's making small angles to the K^+ in the forward or backward direction, since short events might be expected to be missed for this reason more frequently than long ones. Since this cut did not alter the energy dependence of the scanning efficiency, it was deemed unnecessary.

B. Corrections

The corrections made to the τ' spectrum, discussed in (i) through (vi) below, are tabulated by energy bin in Table I. The slope, g , from the fit to a linear spectrum (see Sec. IV for definitions of s_3 and s_0)

$$|M|^2 = 1 + g(s_3 - s_0)/m_{\pi^+}^2$$

and the χ^2 values for the fit for both uncorrected and corrected data are shown in the table to exhibit the shift in slope resulting from the corrections. The last bin was not included in the fits because the corrections are a large percentage of the data for this bin. Two corrections, both very small compared to the statistical error

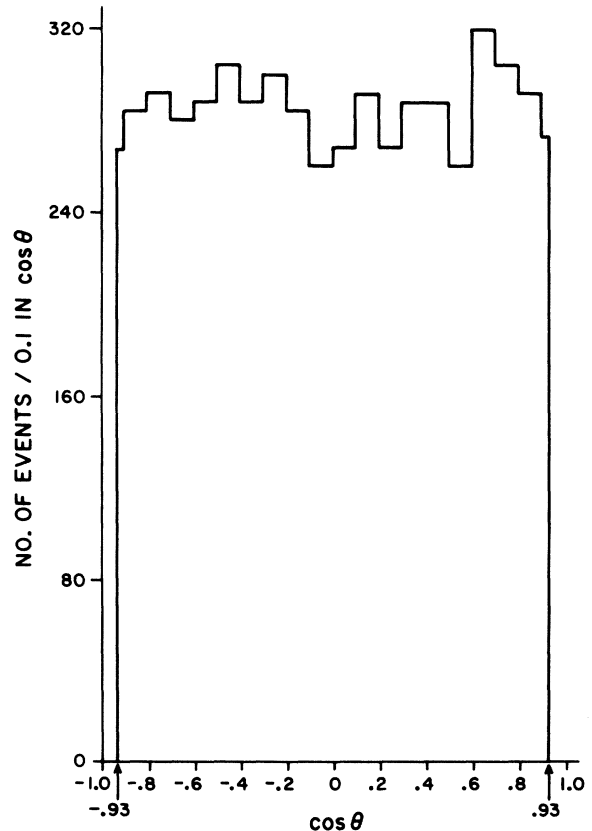


FIG. 3. Cosine of the dip angle distribution of the τ^+ 's.

TABLE I. Corrections to the τ' spectrum.

Energy interval (MeV)	Cut data	Corrections							Cut and corrected data ($K_{\mu 3}$ method 1)	Cut and corrected data ($K_{\mu 3}$ method 2)
		(i) Method 1	(i) Method 2	(ii)	(iii)	(iv)	(v)	(vi)		
8-11	489	-14.2	-11.9	-0.0	-11.2	+1.7	+0.0	+0.0	465.3	467.6
11-14	559	-16.1	-13.6	-0.0	-11.8	+3.0	+0.6	+0.0	534.7	537.2
14-17	540	-18.8	-15.8	-0.0	-11.8	+4.4	+1.8	+0.0	515.6	518.6
17-20	543	-19.8	-16.7	-0.0	-11.8	+6.0	+3.1	+0.0	520.5	523.6
20-23	551	-21.4	-18.0	-0.0	-11.3	+7.6	+4.3	+0.5	530.7	534.1
23-26	496	-24.2	-20.4	-0.0	-10.8	+9.1	+5.3	+0.5	475.9	479.7
26-29	474	-24.7	-20.8	-0.0	-10.2	+10.3	+6.1	+1.3	456.8	460.7
29-32	411	-25.5	-21.5	-0.0	-9.6	+11.2	+6.7	+2.0	395.8	399.8
32-35	376	-27.7	-23.4	-0.0	-8.8	+11.7	+6.9	+3.2	361.3	365.6
35-38	321	-29.9	-25.2	-0.0	-7.8	+11.6	+6.8	+4.3	306.0	310.7
38-41	275	-29.7	-25.0	-0.0	-6.5	+11.0	+6.3	+4.0	260.1	264.8
41-44	232	-29.6	-25.0	-1.3	-5.9	+9.7	+5.5	+4.3	214.7	219.3
44-47	179	-30.3	-25.5	-1.5	-5.2	+7.8	+4.3	+3.8	157.9	162.7
47-50	124	-31.9	-26.9	-2.6	-4.2	+5.4	+2.9	+3.6	97.2	102.2
50-53	65	-34.3	-29.0	-5.4	-4.0	+2.5	+1.3	+1.5	26.6	31.9
Totals	5635	-378.1	-318.7	-10.8	-130.9	+113.0	+61.9	+29.0	5319.1	5378.5
g	0.571								0.601	0.592
χ^2	7.21								4.25	4.27
$\chi^2/D.F.$	0.601								0.354	0.356

in the slope, were applied to the slope after all others, one due to the difference in scan efficiencies across the spectrum, the other due to the inclusion of the events measured by RANGER.

These will be discussed in (vii) and (viii) below.

(i) $K_{\mu 3}$ with apparent μ pips. This correction was actually estimated in two different ways to provide a check on consistency. The two methods agree within errors and differ in the best value of the slope by 0.009, as shown in Table I, which is about one-half the error in the slope due to statistics. Method 1 will be used in quoting results, since it depends only on track measurement and does not involve the decisions of scanners.

Method 1. SHAPE fits each track in several segments and calculates a χ^2 value for goodness of fit for each secondary to the two mass hypotheses π^+ and μ^+ , namely

$$\chi_R^2 = \frac{\sum \text{pieces} [(p_{\text{curv}}^{(i)} - p_{\text{range}}^{(i)})^2] / (\Delta p_{\text{curv}}^{(i)})^2}{\text{No. of pieces}},$$

where $p_{\text{curv}}^{(i)}$ is the momentum by curvature at the center of the i th piece of the track, the pieces being chosen internally by the program to optimize the fit,³ and $p_{\text{range}}^{(i)}$ is the momentum by range at the same point on the track for the given mass hypothesis. The value of $p_{\text{range}}^{(i)}$ is obtained by assuming the track stops and using the range ver-

sus momentum relationships for pions or muons to get the momentum at the center of the i th piece.

A scatter plot of $\chi_R^2(\mu)$ vs $\chi_R^2(\pi)$ is displayed in Fig. 4 for the following: (a) pions from τ decay with kinetic energies > 47 MeV; (b) secondaries which are between 22.5 and 24.5 cm long and which show no evidence for a μ pip at the end resulting from the decay of K^+ 's which meet our stopping criterion; the secondaries are approximately 150 times more likely to be muons than pions; (c) the 189 τ' secondaries in the two highest energy bins plus the 55 secondaries from the consistency check region. The latter events met all τ' criteria and survived all cuts except the cut on range, their ranges falling between 22.5 and 24.5 cm. Below 47 MeV, the values of $\chi_R^2(\mu)$ and $\chi_R^2(\pi)$ did not differ by enough to make a clear separation.

The number of $K_{\mu 3}$ events contained in (c) was estimated by assuming that the fractional number of pions in regions I and II and of muons in regions I and II were the same for the events in (c) as for pions in (a) and muons in (b), respectively. A trial value for the total number of muons in the three energy intervals, N_μ , was chosen, and the corresponding trial value for the total number of pions, N_π , was obtained by subtracting N_μ from the total number of events in (c), or 244. The value of N_μ , N_μ^{min} , which minimized the expression

$$\chi^2_{\mu} = \sum_{i=I,II} \frac{(N_i - f_i^{(b)} N_{\mu} - f_i^{(a)} N_{\pi})^2}{N_i},$$

where N_i is the total number of secondaries in (c) falling in region i and $f_i^{(a)}$ and $f_i^{(b)}$ are the fractional numbers of events in region i on plots (a) and (b), was then used in making the $K_{\mu 3}$ correction by Method 1. The calculated $K_{\mu 3}$ spectral values, choosing $\xi = 0$ and normalizing to a total of N_{μ}^{min} in the three energy intervals represented in Fig. 4, were subtracted from the data in each

bin.

Method 2. A theoretical $K_{\mu 3}$ spectrum for $\xi = 0$ was employed. This was normalized to the observed τ' sample using the following factors:

- (1) the Particle Data Group⁴ values for the branching ratios;
- (2) the probability of detecting a μ -pip on a stopping π^+ , 75.0%, determined from a sample of τ decays;
- (3) the probability of observing a false μ pip on a stopping μ^+ , 6.60%, determined from the

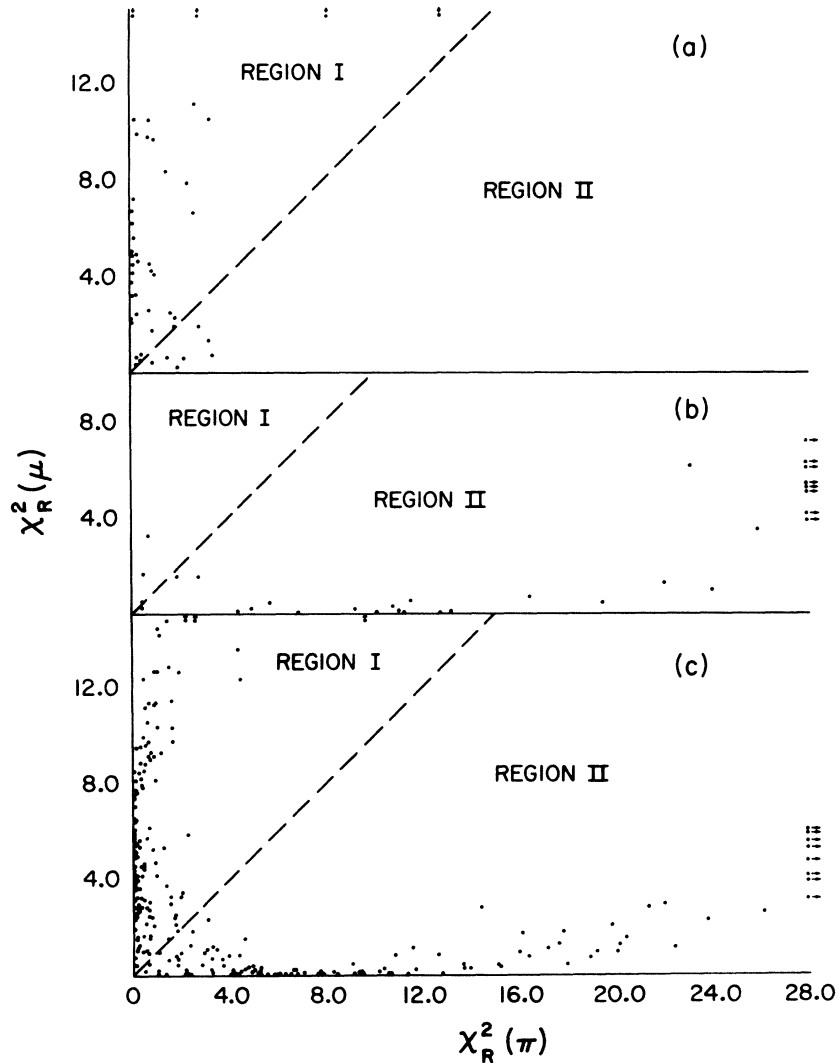


FIG. 4. Scatter plot of $\chi_R^2(\mu)$ versus $\chi_R^2(\pi)$ for the following: (a) π^+ 's from fitted τ events, (b) secondaries which are 150 times more likely to be muons than pions because of the selection criteria, and (c) the secondaries from the two highest energy bins plus the consistency check region above the τ' spectrum selected according to the criteria for this experiment.

sample of $K_{\mu 2}$ events;

(4) corrections to the τ' sample for events outside our range cuts, assuming a slope $g=0.628$;

(5) the correction for $K_{\mu 3}$ contamination determined by Method 1.

This estimate is relatively insensitive to the choice of ξ or g .

(ii) $K\pi_2$ in flight. A Monte Carlo simulation of 115 000 $K\pi_2$ events was made from K^+ 's with the momentum distribution of the 23 in-flight events in the τ background study which passed the K^+ -at-rest cut to determine the fractional number of $K\pi_2$ in each energy bin. For this correction the factors of normalization were the Particle Data Group (PDG) branching ratios and the K^+ in-flight contamination factor.

(iii) K_τ , in flight. The K_τ , in-flight correction was made in exactly the same way as that for the $K\pi_2$ in flight. 23 000 K_τ , in-flight decays were generated by Monte Carlo from K^+ 's with the momentum distribution of the 23 in-flight τ events.

(iv) K_τ , with π^+ scatters $>30^\circ$. In a study of 844 π^+ 's from τ decays, 19 π^+ 's scattered more than 30° . The range to the scatter was measured for each of these and a mean free path calculated assuming that the cross section for nuclear scatters is independent of the momentum for such low-energy pions. The mean free path was found to be 316 cm. The mean free path was used to estimate the loss of events as a function of energy.

(v) K_τ , with π^+ decay in flight. The average velocity of the π^+ 's in each energy bin and the path length traveled in each bin were used to determine the time of flight of the secondaries in the π^+ rest frame. Using the Particle Data Group value for the π^+ lifetime, the number of events lost due to π^+ decay in flight could be calculated.

(vi) K_τ , where the π^+ leaves the bubble chamber. 1208 measured τ decay origins were used as the decay vertices for 120 800 Monte Carlo generated τ' decays. The position of the π^+ ending was estimated by using a function relating chord length in the plane perpendicular to the magnetic field to arc length. If the coordinates of the end point fell outside of a cylindrical surface with radius 1 cm smaller than that of the true bubble chamber radius, the pion was called out. The small difference in radius was chosen because it was felt that a pion decaying so near to the wall would probably not be identified correctly. Similarly, the range component along the magnetic field was used to determine the z coordinate of the end point. If the end-point z lay outside of the planes parallel to the top and bottom glass but 1 cm inside them, the track was called out.

(vii) Corrections to the slope due to range-dependent scan efficiencies. The double-scan ef-

iciencies by energy bin were calculated from the numbers in each bin found only in the first scan, only in the second scan, and in both scans, assuming "equally hard to find events," i.e., that events found in the first scan were no more likely to be found in the second than those missed in the first scan. The number of events in each energy bin for an ideal experiment with a slope of 0.601 and a total of 5292.5 events between 8 and 50 MeV was multiplied by the efficiency factor for that bin, then renormalized to the same total number of events in the spectrum. A least squares fit, using the error in the calculated double-scan efficiencies times the number of events in each bin as weighting factors, gave the best fit value of g to be 0.603. The resulting shift in slope is thus +0.002, and therefore the correction made to the experimental value of the slope for this reason is -0.002.

(viii) Correction to the slope due to the addition of events measured by RANGER. A sample of 90 events measured both by RANGER and by SHAPE were added, first measured one way and then the other, to the data for an ideal experiment with slope 0.601 in the same proportion as RANGER events were added to the SHAPE-measured τ' data. The sample containing the RANGER measures, which tend to be longer on the average, has a slope which is lower by 0.003. The correction that must be applied to the experimental value is therefore +0.003.

The net correction to the slope due to both (vii) and (viii) is therefore +0.001. This is much smaller than the quoted error in g , ± 0.021 , which was obtained by adding in quadrature the statistical error in g , i.e., Δg for Δ_χ^2 equal to 1, and the error in g which would result from an error of 20% in our method of estimating the $K_{\mu 3}$ correction. The errors in all other corrections are negligible compared to these.

Corrections (vii) and (viii) and the quoted error have been calculated in the same way when quoting the results of fitting to a quadratic matrix element.

IV. RESULTS AND CONCLUSIONS

The differential decay rate for $K \rightarrow 3\pi$ may be parametrized by the expression

$$\frac{d\Gamma(K \rightarrow 3\pi)}{ds_3} \propto |M(s_3)|^2 \phi(s_3),$$

where

$$|M|^2 \propto 1 + g[(s_3 - s_0)/m_{\pi^+}{}^2] + h[(s_3 - s_0)/m_{\pi^+}{}^2]^2.$$

Here $\phi(s_3)$ is the Lorentz-invariant phase-space

factor, $s_i = (\not{p}_K - \not{p}_i)^2$, where \not{p}_K and \not{p}_i are the energy-momentum 4-vectors of the K and the i th pion, $s_0 = \frac{1}{3} \sum_{i=1}^3 s_i$, and the index 3 designates the odd pion in the decay, thus the π^+ in τ' decay. The square of the pion mass is introduced to make the coefficients dimensionless.

Since the variable s_3 is linear in the π^+ kinetic energy T_3 ,

$$s_3 = (m_K - m_3)^2 - 2m_K T_3$$

and

$$s_0 = \frac{1}{3} (m_K^2 + m_1^2 + m_2^2 + m_3^2),$$

the calculations were actually carried out using this variable. The cut and corrected data was divided into 14 intervals each 3 MeV wide between 8 and 50 MeV. Then, the expression for the differential decay rate was numerically integrated to get the expected number of events in each of the 14 energy intervals as a function of the parameters g and h . A χ^2 fit to the data was made, assuming first that the spectrum is linear, i.e., $h=0$. The value of g which minimized χ^2 , corrected for the small effects in III B (vii) and III B (viii), was

$$g = 0.602 \pm 0.021.$$

The χ^2 for this fit was 4.25 for 12 degrees of freedom, which corresponds to a confidence level of 97.8%. The contributions to the error are 0.0175 from the statistical errors in the data points and 0.012 from the estimated error in the $K\mu_3$ background subtraction.

Allowing for a value of h different from 0 did not result in any significant improvement in the fit. We obtained a χ^2 of 4.19 for 11 degrees of freedom, or a confidence level of 96.5% in this case. The (corrected) values of the parameters which minimized χ^2 were

$$g = 0.630 \pm 0.038,$$

$$h = 0.041 \pm 0.030,$$

with

$$c = 0.54,$$

where c is the correlation between g and h , $\langle \delta g \delta h \rangle / \langle \delta g \rangle \langle \delta h \rangle$. Thus, we find no evidence for a quadratic term significantly different from 0.

It should be pointed out that the increase in the linear coefficient when h is allowed to be nonzero results mostly from the corrections due to the energy bias in the scan efficiency and the inclusion of events measured by RANGER, since these corrections add instead of cancel as in the linear case. This is also responsible for approximately one-half the correlation between g and h . While

it is still true that the corrections to g and h due to the scan bias are smaller than the errors in these parameters, here the corrections are more nearly comparable to the statistical error than in the linear case. However, unless the method used in estimating this correction was completely in error, it would not contribute significantly to the errors in the fit parameters.

The data divided by phase space is displayed with the curve corresponding to the best-fit values of the parameters for the linear fit in Fig. 5 and the quadratic fit in Fig. 6. The errors on the data points are statistical only.

The results of our fits are compared to those of other τ' experiments in Table II. While the agreement between the different experiments appears poor, given the quoted errors, we propose that they can be reconciled by observing that the data of Ref. 5 have not been corrected for spurious $K\mu_3$ events, which we found to be the largest source of background. Since the quoted probability for observing $\pi-\mu-e$ decays on known π^+ 's from τ decay (75%) is the same as in this experiment, indicating similar optical conditions, and since the data come from tracks in a bubble chamber filled with C_3F_8 , in which μ tracks from π decays are shorter and therefore more likely to be ambiguous, the correction for $K\mu_3$ would be expected to be at least comparable. The data in Ref. 6, which come from the same film exposure, would appear in terms of our experience to also underestimate this correction. Since a larger $K\mu_3$ correction removes events from the upper bins, increasing the magnitude of g , this could explain the major part of the discrepancy. The present experiment is in good statistical agreement with Ref. 7, in which most of the data come from τ' decays in a hydrogen bubble chamber, and with Ref. 8, in which over half of the data come from fitted τ' events with 3 or 4 converted γ rays. In both of these experiments, the corrections for background contamination are small.

In order to extract useful information from this experiment, the results must be compared to those of experiments involving the other charge modes of $K \rightarrow 3\pi$. The current world averages for these quantities may not represent the best values which could be obtained from the available data since in several cases they are based on weighted means of experiments that may not be statistically compatible. Since the critical study of the various experiments to look for sources of systematic errors which would be required for a more judicious computation of the averages is beyond the scope of this paper, these averages will be used along with our value of g to compute

the five conventional test quantities for the isospin selection rules. The average for g^0 , the slope of the π^0 spectrum in $K_L^0 \rightarrow \pi^+ \pi^- \pi^0$, is particularly suspect, since it comes primarily from two statistically inconsistent results, the experiment of Albrow *et al.*,⁹ which quotes 0.651 ± 0.012 on the basis of 29 000 events and that of Buchanan *et al.*,¹⁰ which quotes 0.555 ± 0.016 for 36 000 K^0 decays. However, a recent experiment by Buchanan *et al.*¹¹ in which the three major decay modes of the K_L^0 were studied simultaneously in a wire chamber magnetic spectrometer quotes a higher value for g^0 , 0.590 ± 0.022 for 56 000 $K_L \rightarrow 3\pi$ decays. Reference 11 also quotes a revised value for the results of Ref. 10, $g^0 = 0.592 \pm 0.022$. Both results tend to corroborate the most recent PDG average 0.610 ± 0.021 . A recent high-statistics experiment by Messner *et al.*,¹² involving 509 000 $K_L \rightarrow \pi^+ \pi^- \pi^0$ decays, quotes $g^0 = 0.636 \pm 0.009$ when fitting to a linear spectrum. We have calculated a new world average using this result and the PDG average for use in the $\Delta I = \frac{1}{2}$ rule tests. The major contribution to g_τ , the slope of the π^\mp in $K^\pm \rightarrow \pi^\pm \pi^\pm \pi^\mp$, comes from the wire spark chamber experiment of Ford *et al.*,¹³ involving 750 000 τ

decays of either sign. The averages used for the slope parameters are

$$g^0 = 0.632 \pm 0.008 \text{ (PDG + results of Ref. 12),}$$

$$g_\tau = -0.214 \pm 0.004 \text{ (PDG).}$$

Table III shows the experimental values for the five conventional test parameters obtained as described above, all of which should equal 0 if a strict $|\Delta I| = \frac{1}{2}$ rule is assumed, along with several theoretical predictions for them. A common feature of all the models shown is that they include both $|\Delta I| = \frac{3}{2}$ and $|\Delta I| = \frac{1}{2}$ in H_W but no $|\Delta I| \geq \frac{5}{2}$ amplitudes. Model A (see Ref. 14) assumes the current-algebra relations and the PCAC (partially conserved axial-vector current) condition which relate the $K \rightarrow 3\pi$ amplitudes to those for $K \rightarrow 2\pi$ at the soft-pion points, and the extrapolation to the physical region for $K \rightarrow 3\pi$ is carried out assuming that the $K \rightarrow 3\pi$ matrix element is linear. Final-state interactions are assumed negligible. Earlier predictions based upon similar models differ only because earlier values for the $K \rightarrow 2\pi$ rates were used.^{15,16} Model B (see Ref. 17) is a phenomenological model due to Holstein. Here, the amplitude is constructed from pion poles,

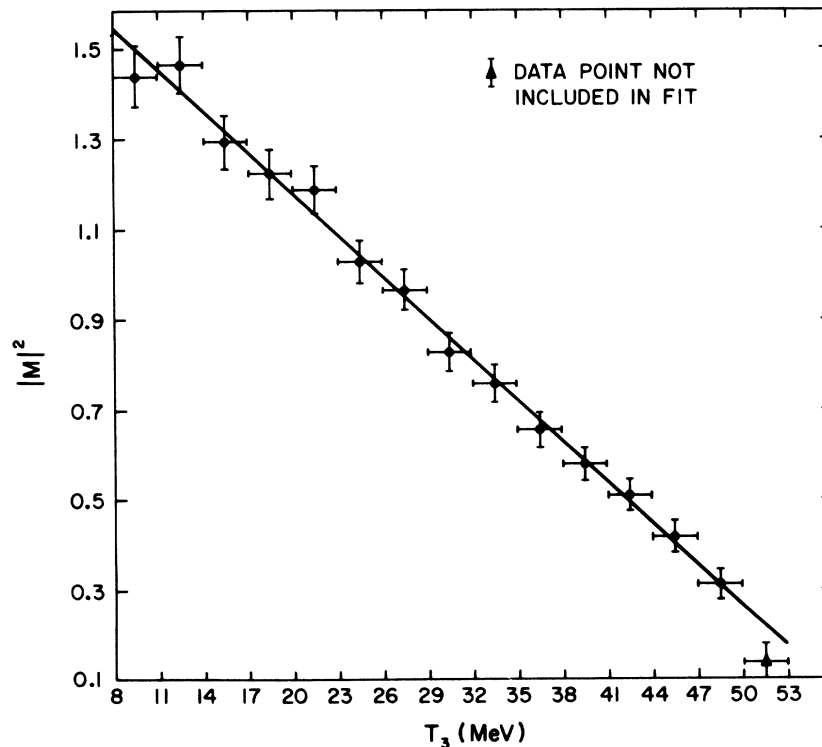


FIG. 5. Distribution in T_3 of the cut and corrected data weighted by phase space for the fit to a linear spectrum of the form $|M|^2 = 1 + g[(s_3 - s_0)/m_{\pi^+}^2]$. The solid curve is $|M|^2$ for $g = 0.602$. Errors displayed are statistical only.

kaon poles, and terms up to first order of an expansion in the momentum of the pions. The amplitude so constructed is required to satisfy the current-algebra relations in the soft-pion limit. The predictions differ slightly from those above since the amplitude contains terms with kinematic factors of order m_π^2/m_K^2 which go to 0 in the soft-pion limit but which make a small contribution in the physical region where the predictions hold. A Veneziano model calculation due to Hara is labeled C.¹⁴ Hara assumes the pion- and kaon-pole dominance model of $K \rightarrow 3\pi$ decays

and constructs the decay amplitude from amplitudes which contain pion and kaon poles plus poles due to higher resonances on the π and K trajectories such that the resulting amplitude satisfies the current-algebra relations at the soft-pion points. The imaginary part of the amplitude is found to be small ($\sim 3\%$) under the assumptions made, so that the decay matrix is still almost linear. Not only are the five test quantities in quite good agreement with experiment but also the calculated numerical values of the slopes, which are

$$\left. \begin{array}{l} g_\tau = -0.24 \\ g_{\tau^+} = 0.62 \\ g^0 = 0.60 \end{array} \right\} \text{to be compared with } \left\{ \begin{array}{l} -0.214 \pm 0.004 \text{ (PDG)} \\ 0.602 \pm 0.021 \text{ (this expt.)} \\ 0.632 \pm 0.008 \text{ (PDG + results of Ref. 12).} \end{array} \right.$$

Hara's predictions for the absolute decay rates are low, however, which he feels might be attributed to off-mass-shell effects. They can be brought into agreement with experiment by as-

suming nonlinear trajectories, but this results in a poorer agreement with the slopes.

The over-all good agreement between the experimental values and these theoretical predic-

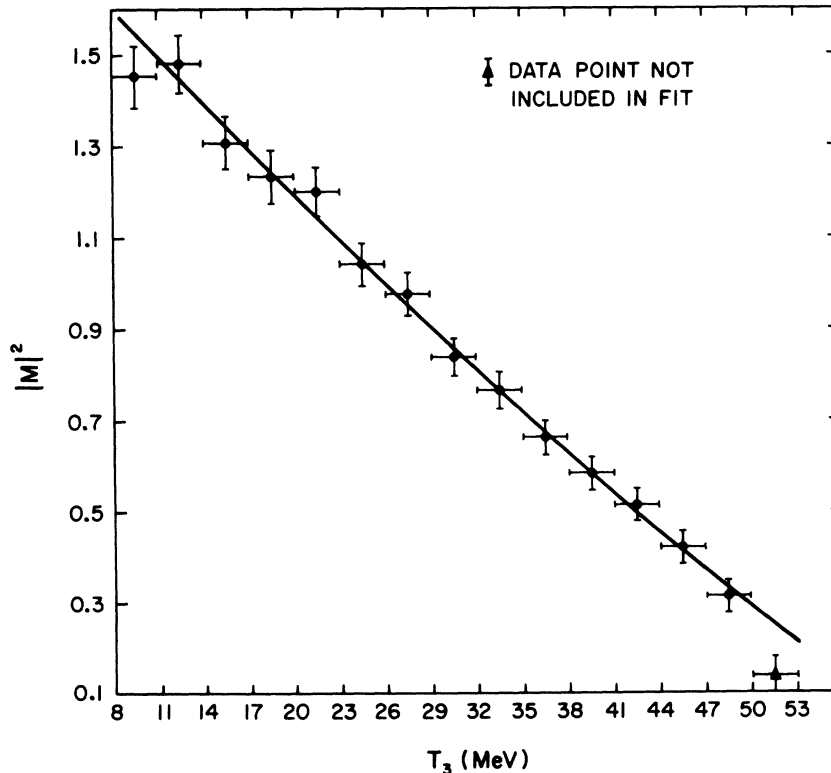


FIG. 6. Distribution in T_3 of the cut and corrected data weighted by phase space for the fit to a quadratic spectrum of the form $|M|^2 = 1 + g[(s_3 - s_0)/m_{\pi^+}^2] + h[(s_3 - s_0)/m_{\pi^+}^2]^2$. The solid curve is $|M|^2$ for $g = 0.630$ and $h = 0.041$. Errors displayed are statistical only.

TABLE III. Tests of isospin selection rules in $K \rightarrow 3\pi$ decays, current experimental values, and recent theoretical predictions.

	Test 1	Test 2	Test 3	Test 4	Test 5
Definition	$\left[\frac{2}{3} \frac{\Gamma_{K^0 \rightarrow \pi^+ \pi^0 \pi^0}}{\phi_{K^0 \rightarrow \pi^+ \pi^0 \pi^0}} \right] - 1$	$\left[\frac{1}{4} \frac{\Gamma_{K^+ \rightarrow \pi^+ \pi^+ \pi^-}}{\phi_{K^+ \rightarrow \pi^+ \pi^+ \pi^-}} \right] - 1$	$\left[\frac{1}{2} \frac{\Gamma_{K^+ \rightarrow \pi^+ \pi^+ \pi^-}}{\phi_{K^+ \rightarrow \pi^+ \pi^+ \pi^-}} \times \left(\frac{\Gamma_{K^0 \rightarrow \pi^+ \pi^+ \pi^0}}{\phi_{K^0 \rightarrow \pi^+ \pi^+ \pi^0}} \right)^{-1} \right] - 1$	$\frac{1}{2} g_{r'} + g_r$	$g^0 + g_r - \frac{1}{2} g_{r'}$
Nonzero value indicates presence of:	$ \Delta I \geq \frac{5}{2}$ transitions to $I = 3$ symmetric state	$ \Delta I \geq \frac{5}{2}$ transitions to $I = 3$ symmetric state	$ \Delta I = \frac{3}{2}$ transition to $I = 1$ symmetric state	$ \Delta I \geq \frac{3}{2}$ transitions to $I = 2$ nonsymmetric state	$ \Delta I = \frac{3}{2}$ transitions to $I = 1$ states of both symmetries
Present experimental values	0.01 ± 0.048 (PDG)	-0.076 ± 0.026 (PDG)	0.190 ± 0.025 (PDG)	0.087 ± 0.012 (PDG and this expt.)	0.117 ± 0.014 (PDG, Ref. 12 and this expt.)
Estimated uncertainty in these values due to e.m. effects	0.1	0.1	0.1	0.01	0.01
Theoretical models					
A Hara Ref. 14, Sec. II.	0	0	0.07	0.09	0.09
B Holstein Ref. 17	0	0	0.23	0.092 ^a	0.103 ^a
C Hara Ref. 14, Sec. V a	0	0	0.13	0.07	0.05

^a Since quoted predictions were in the form of ratios, the value of $g_{r'}$ from this experiment was used to convert to differences.

and especially by the Bubble Chamber crew during the filming of the data at Argonne National Laboratory is gratefully acknowledged. I would like to thank the many scanners and measurers who

worked on this experiment for their effort and cooperation. A special thanks to Priscilla Deibig who spent many hours reexamining events and checking and rechecking lists of events.

*Work supported in part by the U. S. Atomic Energy Commission.

¹S. Weinberg, *Phys. Rev. Lett.* **4**, 87 (1960).

²For a detailed discussion of the $K \rightarrow 3\pi|\Delta I|=\frac{1}{2}$ rule tests, see C. Bouchiat and M. Veltman, in *Proceedings of the Topical Conference on Weak Interactions, CERN, 1969* (CERN, Geneva, 1969), pp. 213-221.

³C. T. Murphy, SHAPE Users' Manual, Part 4 (unpublished).

⁴Particle Data Group (hereafter referred to as PDG), *Phys. Lett.* **50B**, 1 (1974).

⁵D. Davison *et al.*, *Phys. Rev.* **180**, 1333 (1969).

⁶G. E. Kalmus *et al.*, *Phys. Rev. Lett.* **13**, 99 (1964).

⁷V. Bisi *et al.*, *Nuovo Cimento* **35**, 768 (1965).

⁸B. Aubert *et al.*, *Nuovo Cimento* **12A**, 509 (1972).

⁹M. G. Albrow *et al.*, *Phys. Lett.* **33B**, 516 (1970).

¹⁰C. D. Buchanan *et al.*, *Phys. Lett.* **33B**, 623 (1970).

¹¹C. D. Buchanan *et al.*, Johns Hopkins Report No. 7405 (UCLA Report No. 1101), 1974 (unpublished).

¹²R. Messner *et al.*, *Phys. Rev. Lett.* **33**, 1458 (1974).

¹³W. T. Ford *et al.*, *Phys. Lett.* **38B**, 335 (1972).

¹⁴Y. Hara, *Phys. Rev. D* **2**, 376 (1970).

¹⁵C. Bouchiat and Ph. Meyer, *Phys. Lett.* **25B**, 282 (1967).

¹⁶A. D. Dolgov and V. I. Zakharov, *Yad. Fiz.* **7**, 352 (1968) [*Sov. J. Nucl. Phys.* **7**, 232 (1968)].

¹⁷B. Holstein, *Phys. Rev.* **183**, 1228 (1969).

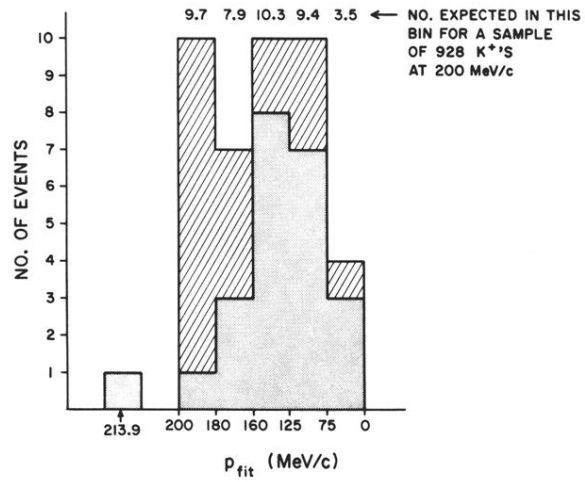


FIG. 2. Momentum distribution of K^+ 's from fitted τ -in-flight events—the shaded region contains the K^+ 's that passed the K^+ -at-rest test ($-14 < p_{range} - p_{curv.} < +30$ MeV/c) and the cross-hatched region those that did not ($p_{range} - p_{curv.} < -14$ MeV/c).